Marine Geology 238 (2007) 75–91
MARINE GEOLOGY
INTERNATIONAL JOURNAL OF MARINE GEOLOGY, GEOCHEMISTRY AND GEOPHYSICS
www.elsevier.com/locate/margeo

Large boulder deposits by tsunami waves along the Ionian coast of south-eastern Sicily (Italy)

Giovanni Scicchitano, Carmelo Monaco *, Luigi Tortorici

Dipartimento di Scienze Geologiche, University of Catania, Corso Italia, 55, 95129 Catania, Italy

Received 30 May 2006; received in revised form 15 December 2006; accepted 23 December 2006

Abstract

The Ionian coast of south-eastern Sicily, between the towns of Augusta and Siracusa, is characterized by the occurrence of anomalous calcareous boulders. They are mostly scattered along large terraces located 2–5 m above sea level, gently sloping towards the sea. Boulders are up to 182 t in weight and are arranged either in isolated elements or small groups composed of a few stacked elements. Several boulders show biogenic encrustations (*serpulids*, *balanids*, *lithophaga*) all over their surface which suggest that they were dragged from the mid-sublittoral zone. Other boulders are partially covered by biogenic encrustations and show morphological features (karstic pools, exposed fracture surfaces) suggesting that they were detached and scattered from the mid-supralittoral zone. Direct observations on each boulder (distance from the shoreline, size and weight), together with statistical analysis of the storm regime of the area, allowed to operate hydrodynamic estimations useful to verify if tsunami or storm waves were responsible for their detachment and transport, while radiocarbon age determinations on marine organisms constrained the timing. Collected data, compared to historical catalogues, suggest that in the last 1000 years three seismic events with local sources could have triggered tsunami waves associated with the boulder deposits occurring in the area. The first two were probably triggered by the earthquakes of February 4, 1169 and January 11, 1693 which destroyed south-eastern Sicily. According to geological data and numerical modelling, the seismogenic source could be located in the Ionian offshore between Catania and Siracusa. The third tsunami was generated by the strong earthquake which took place in the Strait of Messina on December 28, 1908.

Keywords: tsunami; boulder deposits; south-eastern Sicily; Mediterranean Sea

1. Introduction

One of the major effects of tsunamis on rocky coasts is represented by detachment of large boulders in the near-shore zone and their deposition farther inland (Dawson, 1994; Dawson and Shi, 2000; Bryant and Nott, 2001). Large boulder accumulations related to the occurrence of tsunamis have been observed all over the world as along the coasts of Ryukyu Islands in Japan (Nakata and Kawana, 1993), New South Wales and northern Queensland in Australia (Young et al., 1996; Bryant and Nott, 2001) and Southern Caribbean Islands (Scheffers, 2002). In the Mediterranean Sea, large boulder deposits along the coasts of the Messina Straits (Sicily) have been related to the AD 1908 tsunami (Heck, 1947), slabs and boulders of Pleistocene calcarenites, up to 80 t in weight, scattered along the Ionian coast of Apulia (Southern Italy), were related to

* Corresponding author. Fax: +39 095 7195728.
E-mail addresses: g.scicchitano@unict.it (G. Scicchitano), cmonaco@unict.it (C. Monaco), tortoric@unict.it (L. Tortorici).

0025-3227/$ - see front matter
doi:10.1016/j.margeo.2006.12.005

three tsunami events occurred between the 15th and 18th centuries (Mastronuzzi and Sansò, 2000, 2004). According to Kelletat and Schellmann (2002), large volumes of coarse rocky material including boulders weighing over 20 t were moved by tsunamis occurred on Cyprus during the last few centuries.

Identifying bolder deposits and determining wave heights and age of deposition can help to evaluate the magnitude and frequency of tsunamis along coastal areas and therefore to assess coastal hazards. Hydrodynamics of boulder emplacement and transport on shore platform have been dealt with, among others, by Nott (1997, 2003a,b) and Noormets et al. (2004). Nott's approach relates the forces required to transport boulders to wave height and represents an easy tool useful to determine if storm or tsunami waves are responsible for their emplacement (see also Nott, 2004). In Noormets's approach hydrodynamic forces at the low submerged shoreline cliff are computed using design wave characteristics based on linear wave theory and experimental results, considering the local wave climate, near-shore bottom topography and initial fracturing of cliff rocks.

The Ionian coast of south-eastern Sicily (Italy), between the towns of Augusta and Siracusa (Fig. 1), is characterized by the occurrence of deposits of anomalous calcareous boulders. Their surface is usually covered by biogenic encrustations which indicate that they were detached from the mid or sub-littoral zone. In order to verify if the boulders are compatible with the storm wave regime of the area or if tsunami waves were responsible for their detachment, transport and deposition, we applied the simple Nott (2003a,b) approach. Direct observations on each boulder were carried out, regarding size, direction and distance from the shoreline, whereas the unit weight was determined in the laboratory. As this approach also depends on the pre-transport environment, the probable setting (submerged, sub-aerial, etc.) prior to transportation has been determined. Moreover, detailed submerged profiles of the four coastal sites have been carried out by direct scuba surveying. Finally, radiocarbon age determinations on marine organisms constrained the deposition timing. Collected data have been compared to historical catalogues (Soloviev, 1990; Soloviev et al., 2000; Tinti et al., 2004) to verify if seismic events with local sources could have triggered tsunami waves associated with the boulder deposits occurring in the area.

2. Geological setting

South-eastern Sicily is one of the most seismically active areas of the central Mediterranean (Fig. 1). This area, mostly constituted by the Hyblean Plateau, represents the emerged foreland of the Siculo-Maghrebian thrust belt and is characterized by a continental crust overlain by thick Mesozoic to Quaternary carbonate sequences and volcanics (Grasso and Lentini, 1982; A.A.V.V., 1987). The Ionian sector of the Hyblean Plateau is located on the footwall of a large normal fault system which since the Middle Pleistocene (Bianca et al., 1999) has reactivated the Malta Escarpment, a Mesozoic boundary separating the continental domain from the oceanic crust of the Ionian basin (Scandone et al., 1981; Makris et al., 1986; Sartori et al., 1991; Argnani and Bonazzi, 2005).

Active faulting contributes to a continuous extensional deformation from eastern Sicily to western Calabria (Siculo-Calabrian rift zone, Fig. 1; Monaco et al., 1997; Monaco and Tortorici, 2000). The ESE–WNW extension direction is deduced from structural analysis (Tortorici et al., 1995; Monaco et al., 1997; Jacques et al., 2001), seismological data (Cello et al., 1982; Gasparini et al., 1982; Anderson and Jackson, 1987; CMT, 1976–2006; RCMT, 1997–2006 catalogues) and from VLBI (Ward, 1994) and GPS (D'Agostino and Selvaggi, 2004) velocity fields. In eastern Sicily the normal fault system is mostly located offshore and controls the Ionian coast from Messina to the eastern lower slope of Mt. Etna, joining southwards to the system of the Malta Escarpment (Fig. 1). It is marked by a high level of crustal seismicity producing earthquakes with intensities of up to XI–XII MCS and $M \sim 7$, such as the 1169, 1693 and 1908 events (Baratta, 1901; Postpischl, 1985; Boschi et al., 1995). Several earthquake-generated tsunamis struck the Ionian coast of south-eastern Sicily in historical times (AD 1169, 1329, 1693, 1818, 1908, 1990; Tinti et al., 2004; see Table 1). According to published geological data and numerical modelling, the seismogenic source of these events should be located in the Messina Straits and in the Ionian offshore (the Malta Escarpment) between Catania and Siracusa (Baratta, 1910; Barbano and Cosentino, 1981; Carbone et al., 1982; Postpischl, 1985; Barbano, 1985; Lombardo, 1985; Ghisetti, 1992; Valensise and Pantosti, 1992; Piatanesi and Tinti, 1998; Bianca et al., 1999; Monaco and Tortorici, 2000; Azzaro and Barbano, 2000; Tinti and Armigliato, 2003).

As regards the geomorphology, being the area located on the footwall of a large normal fault system of the Siculo-Calabrian rift zone (Fig. 1), the vertical component of deformation has been recorded by several orders of Middle-Upper Quaternary marine terraces and palaeo-shorelines (Bianca et al., 1999). In particular, the detected boulder deposits usually occur on large surfaces gently sloping towards the sea, bordered by up to 5 m high cliffs, represented by Pleistocene depositional terraces or uplifted wave-cut platforms dissecting Miocene limestones. Along the shore platforms, both Miocene and Pleistocene limestones show sub-horizontal 0.5–1.0 m thick layering, affected by NW–SE and NNW–SSE striking fractures and faults (Adam et al., 2000). It is worth to note that the boulders are preferentially accumulated on sectors of promontories exposed towards north-east (Fig. 2), where the offshore source areas of earthquakes are located (active faults in the Messina Straits and at the foot of the Malta Escarpment, see Fig. 1).

3. Boulder deposits along the Ionian coast of south-eastern Sicily

Boulder deposits have been detected along the Ionian coast of south-eastern Sicily between the towns of Augusta and Siracusa (Fig. 1). Further on four distinct sites will be described from the north to the south, Mt. Tauro peninsula

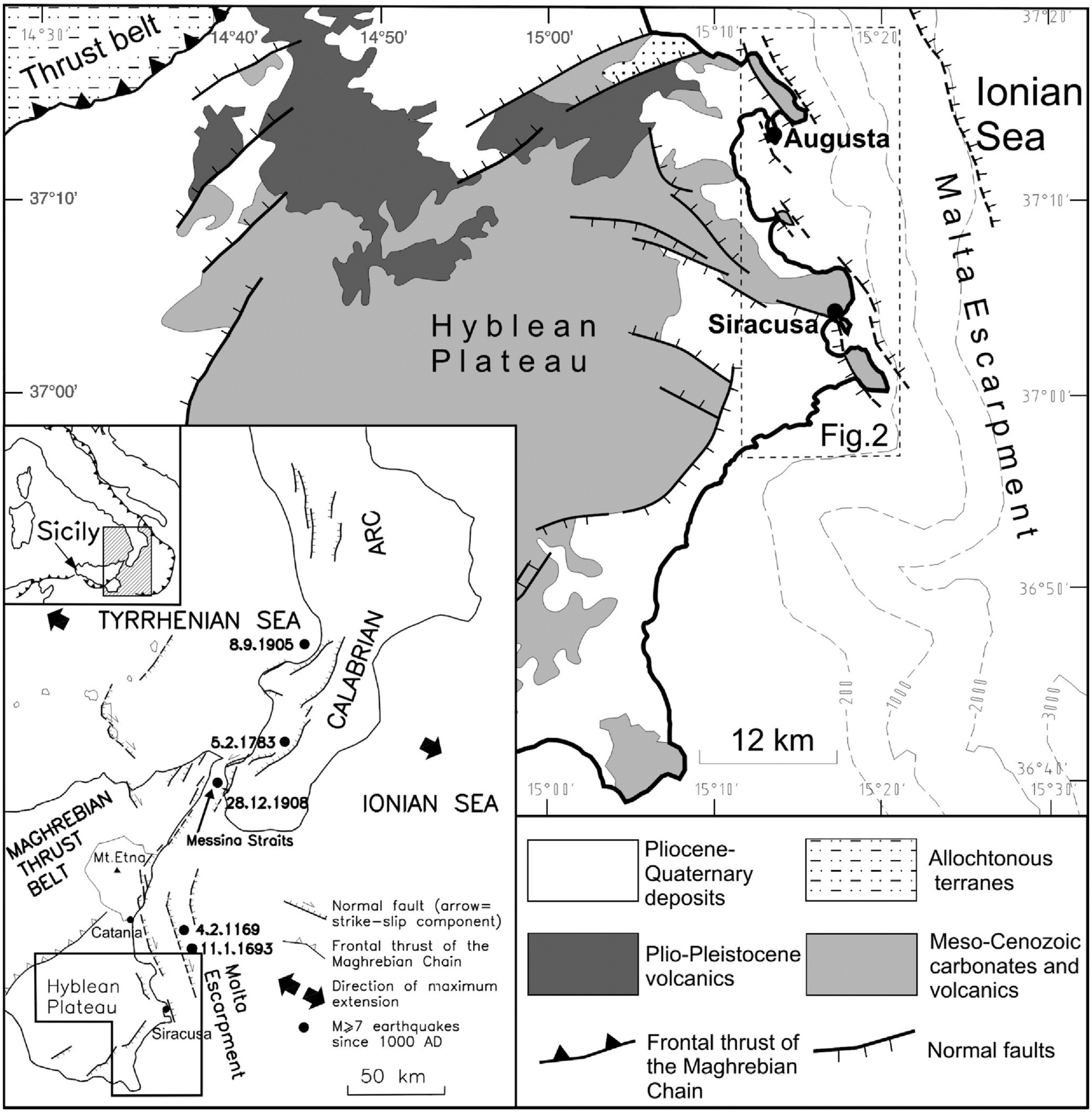

Fig. 1. Tectonic sketch map of south-eastern Sicily. Inset shows the seismotectonic features of the Siculo-Calabrian rift zone (Monaco et al., 1997; Monaco and Tortorici, 2000) and its location in the central Mediterranean area (line with triangles indicates the frontal thrust of the orogenic belt).

Table 1
Tsunami occurred in the Ionian coast of south-eastern Sicily during the last millennium according to the catalogue of Tinti et al. (2004)

Id_Code	Year	Month	Day	Subregion	Reliability	Cause	Earthquake Intensity	Earthquake magnitude	Tsunami Intensity
3	1169	2	4	Eastern Sicily	4	ER	10	6.6	4
4	1329	6	28	Eastern Sicily	2	VA			3
14	1693	1	9	Eastern Sicily	2	ER	8.5	6	2
15	1693	1	11	Eastern Sicily	4	ER	11	7.4	5
38	1818	2	20	Eastern Sicily	4	EA	9	6	2
54	1908	12	28	Messina Straits	4	ER	11	7.2	6
66	1990	12	13	Eastern Sicily	4	ER	7	5.7	2

Reliability: 0 very improbable; 1 improbable; 2 questionable; 3 probable; 4 definite. Cause: EA earthquake associated; VA volcano associated; ER submarine earthquake. Intensity of tsunami: 1 very light; 2 light; 3 rather strong; 4 strong; 5 very strong; 6 disastrous.

and Magnisi peninsula near Augusta, Maddalena Peninsula and Ognina, south of Siracusa (Fig. 2). In order to apply hydrodynamic estimations, direct observations were made on each boulder consisting in size (m) (A-axis>B-axis>C-axis), distance from the shoreline (m) and azimuthal angle of the A-axis. The unit weight of rocks was determined in the laboratory (Table 2).

The boulders generally consist of slabs of Miocene or Pleistocene calcarenites (A.A.V.V., 1987) and are arranged either in isolated elements or small groups sometimes composed of a few stacked elements. Several boulders show biogenic encrustations (*serpulids*, *balanids*, *lithophaga*) all over their surface which suggest that they were dragged from the mid-sublittoral zone. Other boulders are partially covered by biogenic encrustation and show morphological features (karstic pools, exposed fracture surfaces) suggesting that they were carved out along strata planes and joints in the mid-supralittoral zone (see below). Determination of these features is necessary to reconstruct the pre-transport environment of coastal boulders as required by the hydrodynamic approach of Nott (2003a,b).

3.1. Mt. Tauro Peninsula

The Mt. Tauro Peninsula is a calcareous horst located north-east of the Augusta Gulf (Figs. 2 and 3). Few boulders have been found at the south-eastern promontory of this peninsula, that protects from the north-eastern storm waves the Augusta harbour, one of the major oil terminals in the Mediterranean Sea. In particular, large isolated slabs of Miocene calcarenites (unit weight=2.13 g/cm^3) are scattered at a distance of up to 35 m from the coast on a flat terrace (Fig. 4a), located at 2–3 m a.s.l. and gently sloping seawards. The shoreline is constituted by a steep cliff and the near-shore sea bottom topography is irregular, being characterized by three steps at −6/−9 m, −9/−11 m and −11/−30 m (see profile in Fig. 3). The boulders are smoothed and completely covered by biogenic encrustations, suggesting a submerged pre-transport location. The largest boulder (Mag I, Figs. 3 and 4a) shows approximate size of 8×5×0.7 m, with a volume of 28 m^3 and weight of 59.64 t (see Table 2).

3.2. Magnisi Peninsula

The Magnisi Peninsula is located in the middle of the Augusta Gulf, south of the harbour (Figs. 2 and 5). It is formed by a flat and low (maximum 20 m a.s.l.) horst gently tilted to the ENE, constituted by fractured Miocene calcarenites (unit weight=2.13 g/cm^3) and linked to the dry land by a Holocene tombolo. In this site, either isolated large boulders of 8–16 t in weight (Fig. 4b, c) and boulder accumulations composed of single element of maximum 2.5 t in weight are scattered on a rocky platform placed between 5 and 2 m a.s.l., gently sloping to the sea. Seawards, the near-shore sea bottom topography is characterized by a regular slight slope joining to a sandy plane placed at a depth of −12 m (see profile in Fig. 5). In Table 2 the size, weight and distance from the coast of the single boulders are reported. The distribution of A-axis direction ranges between N130 and N160. Absolute age determination by radiocarbon method was carried out on a sample of *serpulid* (Fig. 4d) collected from the boulder MT IX (see below).

The detailed morphological analysis of blocks revealed the general occurrence of exposed fracture surfaces on at least two sides. On the contrary, the other sides are characterized by *balanid* and *serpulid* encrustations, *lithophaga* holes (Fig. 4c, d) or by karstic rock pools on sloping floors (the upper side at first). All these features suggest that they were carved out from the shoreline platform edge (mid-supralittoral zone), along strata planes and joints, and turned over during the transport.

3.3. Maddalena Peninsula

The major boulder accumulation has been found along the north-eastern coast of the Maddalena peninsula, south of the Siracusa natural harbour (Figs. 2 and 6). The

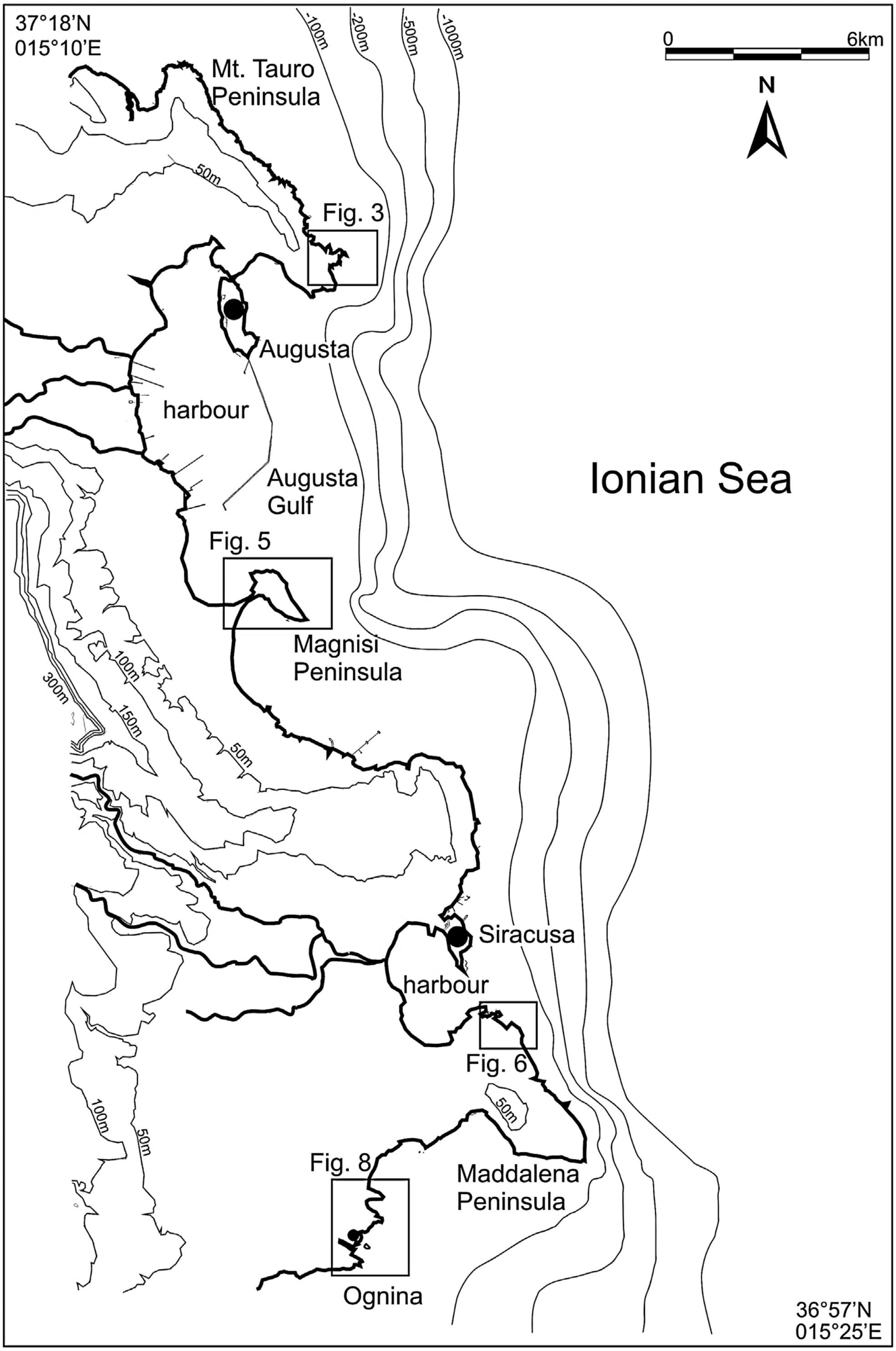

Fig. 2. Geographical position of the studied sites along the Ionian coast of southeastern Sicily, in the Augusta–Siracusa area (see Fig. 1 for location).

peninsula is a calcareous semi-horst gently tilted to the ENE, formed by Miocene sediments that along the coast are unconformably covered by Pleistocene calcarenites (unit weight = 2.28 g/cm^3). Most boulders (Table 2) are up to 40 t in weight and are scattered at a distance of up to 70 m from the coast on a large terrace located 5 m above

Table 2
Size and weight of the boulders surveyed in the Augusta–Siracusa coastal area and tsunami and storm wave heights required to their transport according to the equations of Nott (2003a)

Boulder	Site	Pre-transport setting of the boulder	*A*-axis (m)	*B*-axis (m)	*C*-axis (m)	*A*-axis direction	Vol. (m^3)	ρ_s (g/cm^3)	Weight (t)	Distance from the coast (m)	H_t (m)	H_s (m)
Mag I	Mt. Tauro P.	Submerged	8	5	0.7	N150E	28	2.13	59.64	28	6.82	27.30
MAg II	Mt. Tauro P.	Submerged	4	2.2	0.7	N130E	6.16	2.13	13.12	35	1.60	6.40
MT I	Magnisi P.	Joint bounded	2.3	2	1	N150E	4.60	2.13	9.80	20	3.45	13.80
MT II	Magnisi P.	Joint bounded	2	1.5	0.4	N130E	1.20	2.13	2.56	20	3	12
MT III	Magnisi P.	Joint bounded	2	1.3	0.2	N140E	0.52	2.13	1.11	30	3	12
MT IV	Magnisi P.	Joint bounded	2.7	1	0.4	N150E	1.08	2.13	2.30	30	4.05	16.20
MT V	Magnisi P.	Joint bounded	3.2	0.8	0.2	N150E	0.51	2.13	1.09	30	4.80	19.20
MT VI	Magnesi P.	Joint bounded	3.2	0.8	0.2	N150E	0.51	2.13	1.09	30	4.80	19.20
MT VII	Magnisi P.	Joint bounded	3.2	1.5	0.8	N160E	3.84	2.13	8.18	30	4.80	19.20
MT VIII	Magnisi P.	Joint bounded	1	0.8	0.5	N130E	0.40	2.13	0.85	33	1.50	6
MT IX	Magnisi P.	Joint bounded	3.4	2	2.1	N140E	7.48	2.13	15.93	33	5.10	20.40
MT X	Magnisi P.	Joint bounded	3	2	1.2	N140E	7.20	2.13	15.34	30	4.5	18
MTXI	Magnisi P.	Joint bounded	1	0.5	0.3	N140E	0.15	2.13	0.32	22	1.50	6
B1	Maddalena P.	Joint bounded	1.7	1.1	0.7	N165E	1.31	2.28	2.99	30	2.89	11.59
B2	Maddalena P.	Submerged	3.6	2.6	0.6	N140E	5.62	2.28	12.81	30	2.68	10.74
B3	Maddalena P.	Submerged	10	8	1	N140E	80	2.28	182.40	45	12.37	49.48
B4	Maddalena P.	Submerged	4.9	3.5	1	N040E	17.15	2.28	39.10	35	3.04	12.16
B5	Maddalena P.	Submerged	3.2	2.2	0.5	N150E	3.52	2.28	8.03	35	2.31	9.26
B6	Maddalena P.	Submerged	2.2	1.1	0.3	N000E	0.73	2.28	1.66	55	1.05	4.21
B7	Maddalena P.	Submerged	1.5	1	0.5	N020E	0.75	2.28	1.71	50	0.54	2.17
B8	Maddalena P.	Submerged	3.2	1.6	0.2	N090E	1.02	2.28	2.33	35	2.86	11.45
B9	Maddalena P.	Joint bounded	5.5	2.5	1	N150E	13.75	2.28	31.35	40	9.37	37.50
B10	Maddalena P.	Submerged	1.6	1.6	0.2	N040E	0.51	2.28	1.16	35	2.27	9.07
B11	Maddalena P.	Submerged	3	2	1	N060E	6	2.28	13.68	40	1.08	4.34
B12	Maddalena P.	Submerged	1.7	1.6	0.3	N010E	0.82	2.28	1.87	70	1.79	7.16
B13	Maddalena P.	Submerged	5	3.2	1	N040E	16	2.28	36.48	18	2.63	10.51
B14	Maddalena P.	Submerged	3	1.4	0.3	N050E	1.26	2.28	2.87	25	1.66	6.64
B15	Maddalena P.	Submerged	3.5	2	1	N020E	7	2.28	15.96	35	1.10	4.41
B16	Maddalena P.	Submerged	3.5	2	0.4	N020E	2.1	2.28	4.79	35	2.42	9.68
B17	Maddalena P.	Joint bounded	2.7	1.6	0.4	N100E	1.73	2.28	3.94	45	4.60	18.40
B18	Maddalena P.	Joint bounded	1.8	1.2	0.4	N140E	0.86	2.28	1.96	45	3.07	12.27
B19	Maddalena P.	Submerged	4	2.5	0.4	N090E	4	2.28	9.12	35	3.52	14.07
MA I	Ognina	Joint bounded	2	1.2	1.2	N110E	2.88	2.59	7.46	35	4.25	17.02
MA II	Ognina	Submerged	4	1.8	0.5	N150E	3.60	2.59	9.32	25	2.14	8.58
MA III	Ognina	Joint bounded	3	2	0.8	N080E	4.80	2.59	12.43	15	6.38	25.53
MAd I	Ognina	Joint bounded	3	1.8	1	N100E	5.40	2.59	13.99	20	6.38	25.53
MAd II	Ognina	Joint bounded	1.5	1	0.4	N170E	0.60	2.59	1.55	22	3.19	12.76
MAd III	Ognina	Joint bounded	1.2	1	0.7	N160E	0.84	2.59	2.18	22	2.55	10.21
MAd IV	Ognina	Joint bounded	1.2	1	0.7	N105E	0.84	2.59	2.18	25	2.55	10.21
MAd V	Ognina	Joint bounded	1.5	1.2	0.7	N005E	1.26	2.59	3.26	25	3.19	12.76
MAd VI	Ognina	Joint bounded	1.2	1	0.7	N060E	0.84	2.59	2.18	25	2.55	10.21
MAd VII	Ognina	Joint bounded	2.2	1	0.7	N070E	1.54	2.59	3.99	27	4.68	18.72
MAd VIII	Ognina	Submerged	3.4	1.5	0.5	N010E	2.55	2.59	6.60	12	1.52	6.10
MAs I	Ognina	Submerged	3.5	1.5	0.35	N015E	1.84	2.59	4.77	25	2.09	8.37
MAs II	Ognina	Joint bounded	5	3	0.8	N000E	12	2.59	31.08	28	10.63	42.54
MAs III	Ognina	Joint bounded	3.2	3	2	N010E	19.20	2.59	49.73	25	6.80	27.23
MAsg I	Ognina	Submerged	4	1.4	1.2	N010E	6.72	2.59	17.40	28	0.64	2.40
MAsg II	Ognina	Submerged	5	3	0.8	N005E	12	2.59	31.08	20	3.55	14.20
MAsg III	Ognina	Submerged	3	2	0.4	N070E	2.40	2.59	6.22	20	2.92	11.68
MAsdg I	Ognina	Submerged	2.5	1.5	0.7	N090E	2.63	2.59	6.81	22	1.092	4.37
MAsdg II	Ognina	Submerged	2.2	1.6	0.6	N070E	2.11	2.59	5.46	20	1.38	5.51
MAsdg III	Ognina	Submerged	2.2	1.5	0.7	N080E	2.31	2.59	5.98	22	1.07	4.31
MAsdg IV	Ognina	Submerged	2.2	1.2	0.4	N090E	1.06	2.59	2.75	22	1.19	4.76
MOg I	Ognina	Joint bounded	2.2	1.2	0.7	N090E	1.85	2.59	4.79	33	4.68	18.72
MOg II	Ognina	Joint bounded	1	0.9	0.4	N090E	0.36	2.59	0.93	33	2.13	8.51

sea level, gently sloping towards the sea (Fig. 7a). The shoreline is marked by a steep cliff down to −5 m; the near-shore sea bottom topography is irregular, being characterized by two steps at −6/−10 m and at −10/−32 m (see profile in Fig. 6). The blocks are mostly arranged in isolated elements (Fig. 7b, c) and have also been found on a flat anthropogenic platform at 1–2 m a.s.l. inside an ancient Greek quarry (Fig. 7c) located along the coast (B11–B15 in Fig. 6). Locally, small groups composed of stacked elements occur. In this site a very large boulder (B3), characterized by a volume of 80 m^3 and weight of 182 t, has been found at a distance of 45 m from the coast (Figs. 3 and 7d). According to our observations, during the winter 2006 the boulder B6 was removed inland for about 3 m by storm waves. As regards the distribution of the *A*-axis direction, it is more dispersed around NNE–SSW and SSE–NNW orientations. Samples of *serpulids* and *balanids* were collected from six distinct blocks and their age determined (see below).

The detailed morphological analysis of blocks revealed the occurrence of exposed fracture surfaces on at least two sides of boulders B9, B17, B18 which are characterized by *balanid* and *serpulid* encrustations on the other sides. This suggests that they were carved out from the shoreline platform edge (midlittoral zone), along strata planes and joints. The boulder B1 (Fig. 7b) show also karstic rock pools on the upper side which suggests that it was carved out and dragged from the mid-supralittoral zone. However, most of the boulders are smoothed (Fig. 7d) and completely encrusted by marine organisms living in the mid-infra littoral zone as *serpulids*, *balanids* and *lithophaga*. These features indicate a submerged pre-transport setting. The location of boulders B11–B15 inside an ancient Greek quarry (Figs. 6 and 7c) suggests that they could be relics of quarry operation, even though their morphological features and biogenic encrustations are indicative of a submerged pre-transport setting.

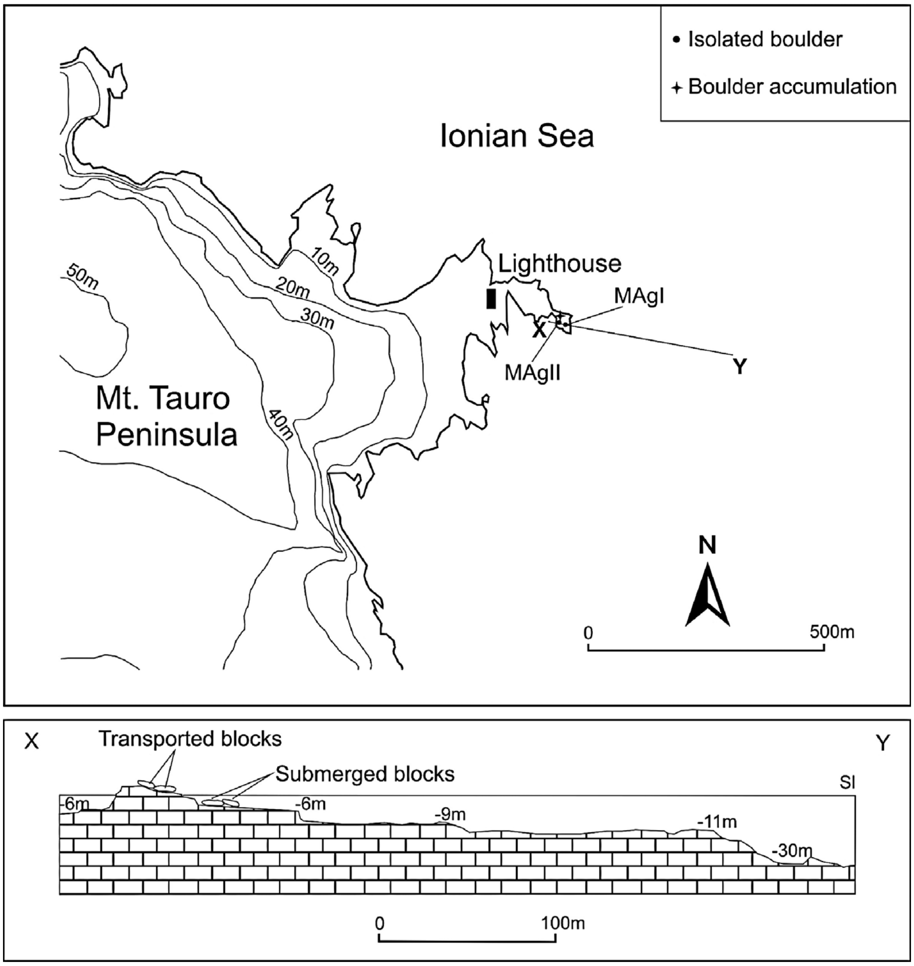

Fig. 3. Position of boulders surveyed at the Mt. Tauro Peninsula (see Fig. 2 for location) and submerged profile showing the near-shore sea bottom topography.

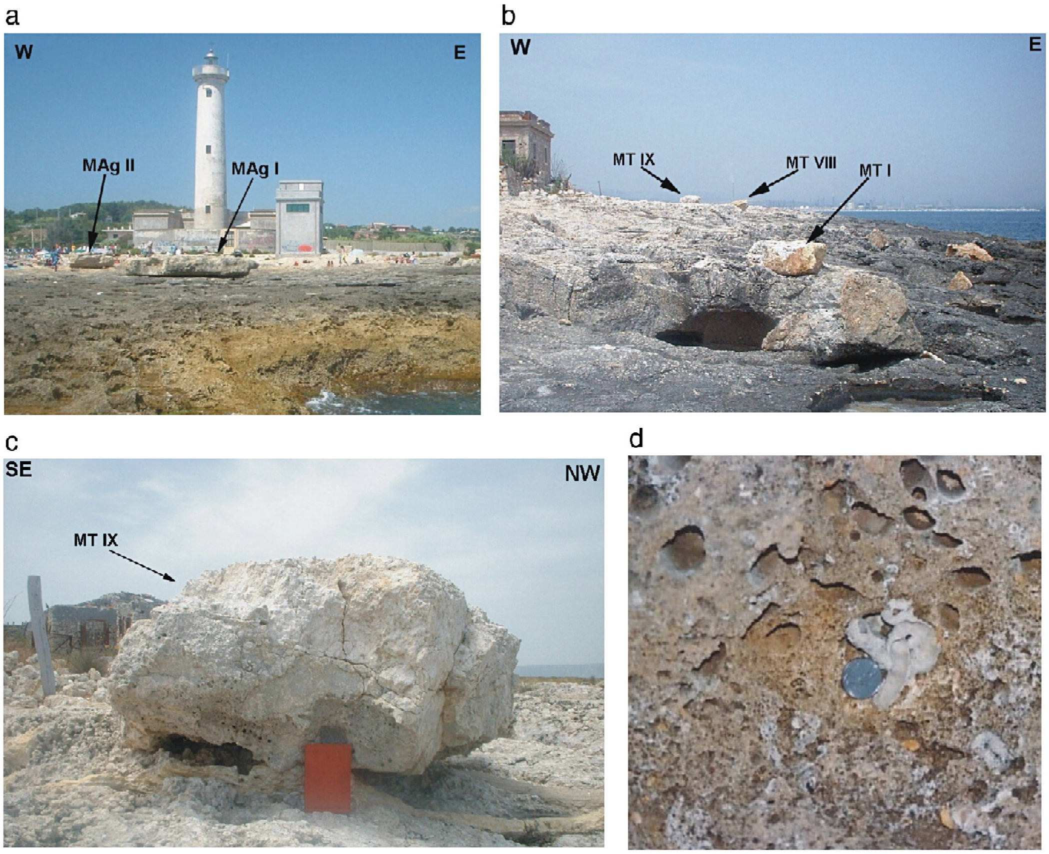

Fig. 4. (a) View of the boulders MAg I and MAg II located at the south-eastern promontory of Mt. Tauro Peninsula (see Fig. 3 for location); (b) scattered boulders deposited on a rocky platform in the north-eastern sector of the Magnisi Peninsula (see Fig. 5 for location); (c) view of the boulder MT IX with evident *lithophaga* holes; (d) *serpulid* encrustation on the boulder MT IX.

3.4. Ognina

The southernmost accumulations were found on three small promontories located in the Ognina area, a tourist settlement located 10 km south of Siracusa (Figs. 2 and 8). The coast is mostly characterized by rocky platforms gently sloping seaward (Fig. 7e), carved on Pleistocene calcarenites (unit weight = 2.59 g/cm^3) and placed between 0.5 and 3 m a.s.l. Seawards, the near-shore sea bottom topography is characterized by a nearly regular slight slope down to −9 m and by a step at −12/−21 m (see profile in Fig. 8). In this site, scattered at a distance of up to 35 m from the coast, are present isolated large boulders, boulder accumulations (Fig. 7f) and imbricated slabs (Fig. 7e), composed of single calcareous elements of 1–50 t in weight (Table 2). The distribution of the *A*-axis direction is dispersed around NNE–SSW and E–W orientations. Absolute age determination by radiocarbon method was carried out on a sample of *serpulid* collected from the boulder MAS II (see below).

The determination of pre-transport setting revealed the occurrence of both submerged and joint bounded blocks (Table 2). Most boulders show exposed fracture surfaces on at least two sides and *balanid* and *serpulid* encrustations or *lithophaga* holes on the other sides (Fig. 7e, f), suggesting that they were carved out from the shoreline platform edge (mid-littoral zone), along strata planes and joints. Some boulders (see MA III in Fig. 7f) show also karstic rock pools on sloping floors, suggesting that they were detached from the mid-supralittoral zone and turned over during the transport. Other boulders show typical features of submerged pre-transport setting, being smoothed and completely encrusted by marine organisms living in the mid-infra littoral zone.

4. Analysis of data

4.1. Tsunami- or storm-generated waves?

In order to determinate whether tsunami- or storm-generated waves were responsible for the deposition of

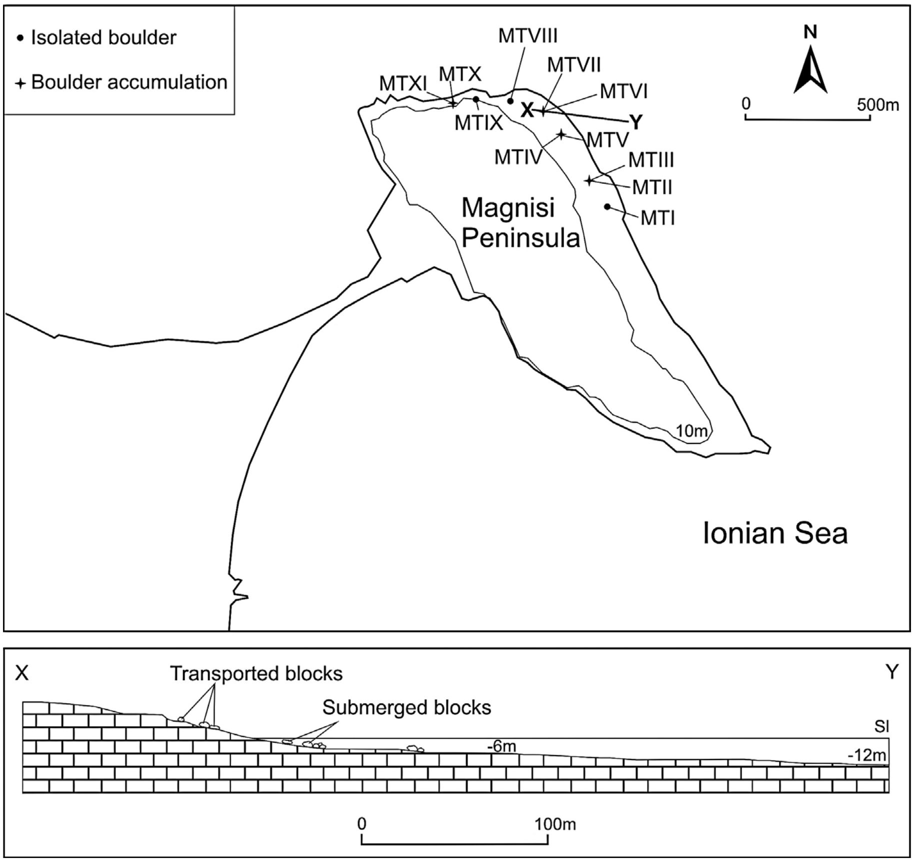

Fig. 5. Position of boulders surveyed at the Magnisi Peninsula (see Fig. 2 for location) and submerged profile showing the near-shore sea bottom topography.

large isolated boulders or fields of boulders on shore platforms, it is necessary to determine the height of the wave required for them to be transported and verify if this is compatible with the storm-wave regime of a coastal area. Nott (1997) developed hydrodynamic equations that relate the forces required to transport coastal boulders to wave height. These equations are limited in their usefulness as they consider only boulders lying loose in shallow water that are lifted and transported in suspension. Boulders can also be transported by waves from sub-aerial positions or can be detached from the shore platform edge where they stand as joint bounded blocks. According to Nott (2003a,b), different forces act on a boulder impacted by a wave depending upon the pre-transport position. A boulder submerged will experience drag and lift forces when impacted by a wave and it will resist movement through the force of restraint compensated by buoyancy, a sub-aerial block also experiences an inertia force, whereas a joint bounded block will only experience lift and drag force (Nott, 2003a). Moreover, substantial fracturing in the rock body is required in order to quarry large clasts from the platform edge (Noormets et al., 2004).

In our study only blocks that were submerged or joint bounded prior to transportation have been identified (Table 2). The detachment of lithic blocks from their joint bounded position on shore platform was favoured by the diffuse layering and fracturing. So, in order to determine the minimum height required by tsunami or storm waves to make them capable of initiating the transportation of boulders we applied Nott's (2003a) equations which for a submerged boulder scenario are simplified as:

$$H_t \geq [0.25(\rho_s - \rho_w/\rho_w)2a]/[c_d(ac/b^2) + c_l]$$

$$H_s \geq [\rho_s - \rho_w/\rho_w)2a]/[c_d(ac/b^2) + c_l]$$

and for a joint bounded block scenario are simplified as:

$$H_t \geq [0.25(\rho_s - \rho_w/\rho_w)a]/c_l$$

$$H_s \geq [(\rho_s - \rho_w/\rho_w)a]/c_l$$

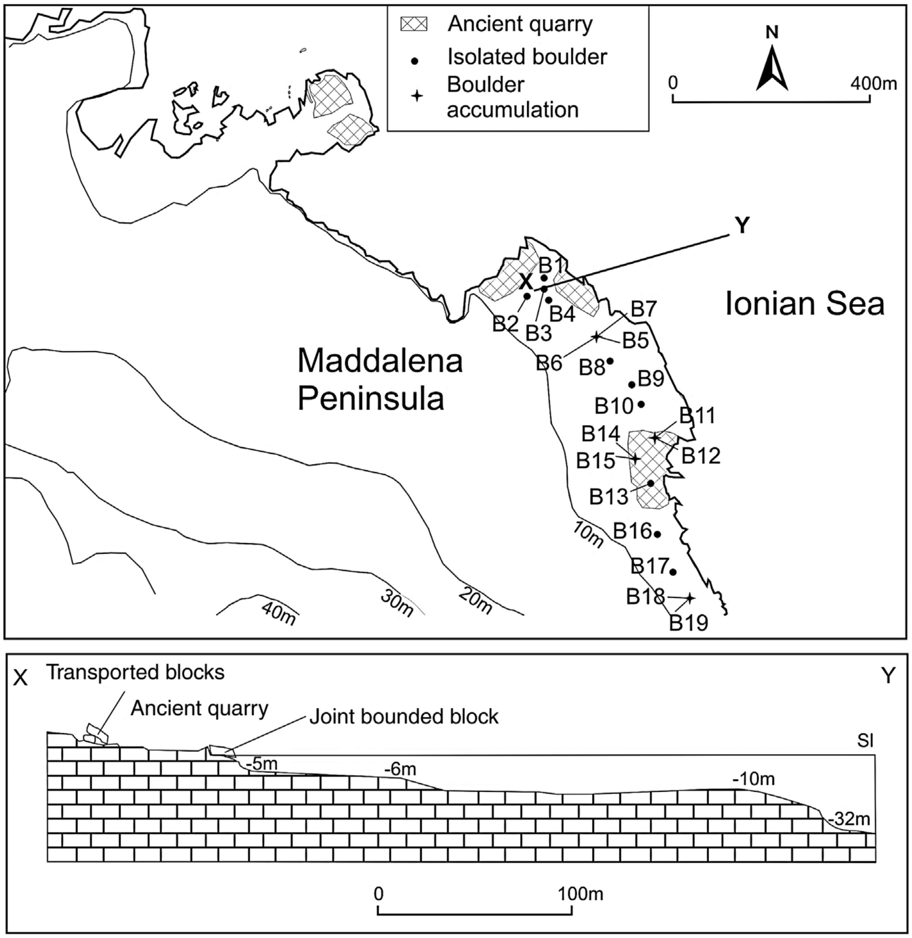

Fig. 6. Position of boulders surveyed at the Maddalena Peninsula (see Fig. 2 for location) and submerged profile showing the near-shore sea bottom topography.

where H_t is the tsunami wave height and H_s is the storm wave height at breaking point, ρ_w is the density of water at 1.03 g/ml, ρ_s is the density of boulder (see Table 2), C_d the coefficient of drag (typically 2), C_l the coefficient of lift (typically 0.178), a, b and c are the A-, B- and C-axis of the boulders. It should be noted that a tsunami wave only needs to be approximately one-quarter the size of a storm wave to transport the same size boulder at the shore. Moreover, the forces necessary to entrain boulders are very sensitive to the thickness (Bryant, 2001): the thinner the boulder, the greater the wave height required to initiate movement. Applying these equations to the deposits detected in the Augusta–Siracusa area it is possible to calculate storm wave heights variable from 2.40 m to 49.48 m and tsunami wave heights variable from 0.54 to 12.37 m (Table 2).

The H_s value calculated for each boulder with Nott's equations should be compared with the wave height (H_b) at breaking point of the studied coastal areas, which can be estimated on the basis of the wave characteristics measured in deep water. According to Sunamura and Horikawa (1974), knowing the wave height and period in deep water, it is possible to calculate the wave height at breaking point of a coastal area by the following equation:

$$H_b/H_o = (\tan\beta)^{0.2}(H_o/L_o)^{-0.25}$$

where H_b is the breaking wave height, H_o the wave height in deep water, β is the slope of sea bottom in the coastal area, L_o the wave length in deep water ($L_o = gT^2/2\pi$; Sarpkaya and Isaacson, 1981).

For the Ionian coast of Sicily significant wave heights (H_o) and periods (T), recorded during the last 18 year by the Catania buoy (RON — Rete Ondametrica Nazionale; www.idromare.com), are available. So, it is possible to calculate the maximum height of the breaking waves occurred in our area at least since 1989. Wave data recorded by the Catania buoy indicate that the most severe

Fig. 7. (a) Scattered boulders deposited on a rocky platform in the north-eastern sector of the Maddalena Peninsula (see Fig. 6 for location); (b) view of the boulder B1 with evident exposed fracture surface and karstic rock pools on its upper side; (c) view of the boulder B13 transported inside an ancient Greek quarry; (d) view of the largest boulder B3; (e) imbricated boulders at Ognina locality (see Fig. 8 for location); (f) view of the boulder MAIII at Ognina locality with evident overturned rock pools.

storm, occurred on February 2, 1996, was characterized by waves with H_o=6.2 m (Fig. 9a) and peak period T=11.3 s (Fig. 9b), moving in a N60E direction. Different values of mean sea bottom slope were determined for the studied coastal sites along the mean direction of extreme waves (N100E) statistically estimated by Inghilesi et al. (2000) for the Catania sector on the basis of RON measurements. Values varying between 2.6° and 5.7° (Table 3), from −100 m depth (half of the maximum L_o estimated for this coastal area) to the shoreline, were obtained combining the bathymetry traced on the official nautical maps (Istituto Idrografico della Marina, 1998) with the detailed submerged profiles (see Figs. 3, 5, 6, 8) carried out by direct scuba surveying.

Processing data with the equation proposed by Sunamura and Horikawa (1974), breaking wave heights $H_{b\ (RON)}$=8.11–9.31 m have been obtained for the analysed coastal areas (Table 3). In order to obtain values of significant wave heights corresponding to longer return periods (up to 50 years) we applied the statistical analysis proposed by Inghilesi et al. (2000). According to this model, the return value $H_{o\ (50)}$ corresponding to return period of 50 years in the Catania sector do not exceed 6.24 m, similar to that measured by the Catania buoy during the last 18 years (H_o=6.2 m). However, we processed also this value with the equation proposed by Sunamura and Horikawa (1974), obtaining breaking wave heights slightly higher ($H_{b\ (50)}$=8.15–9.36 m; see Table 3) than those obtained by 18-year buoy measurements. In our opinion, these values can be considered characteristic of the storm wave regime of the Ionian coast of south-eastern Sicily.

Comparing both the $H_{b\ (RON)}$ and $H_{b\ (50)}$ values with those calculated for each boulder with Nott's equations, it

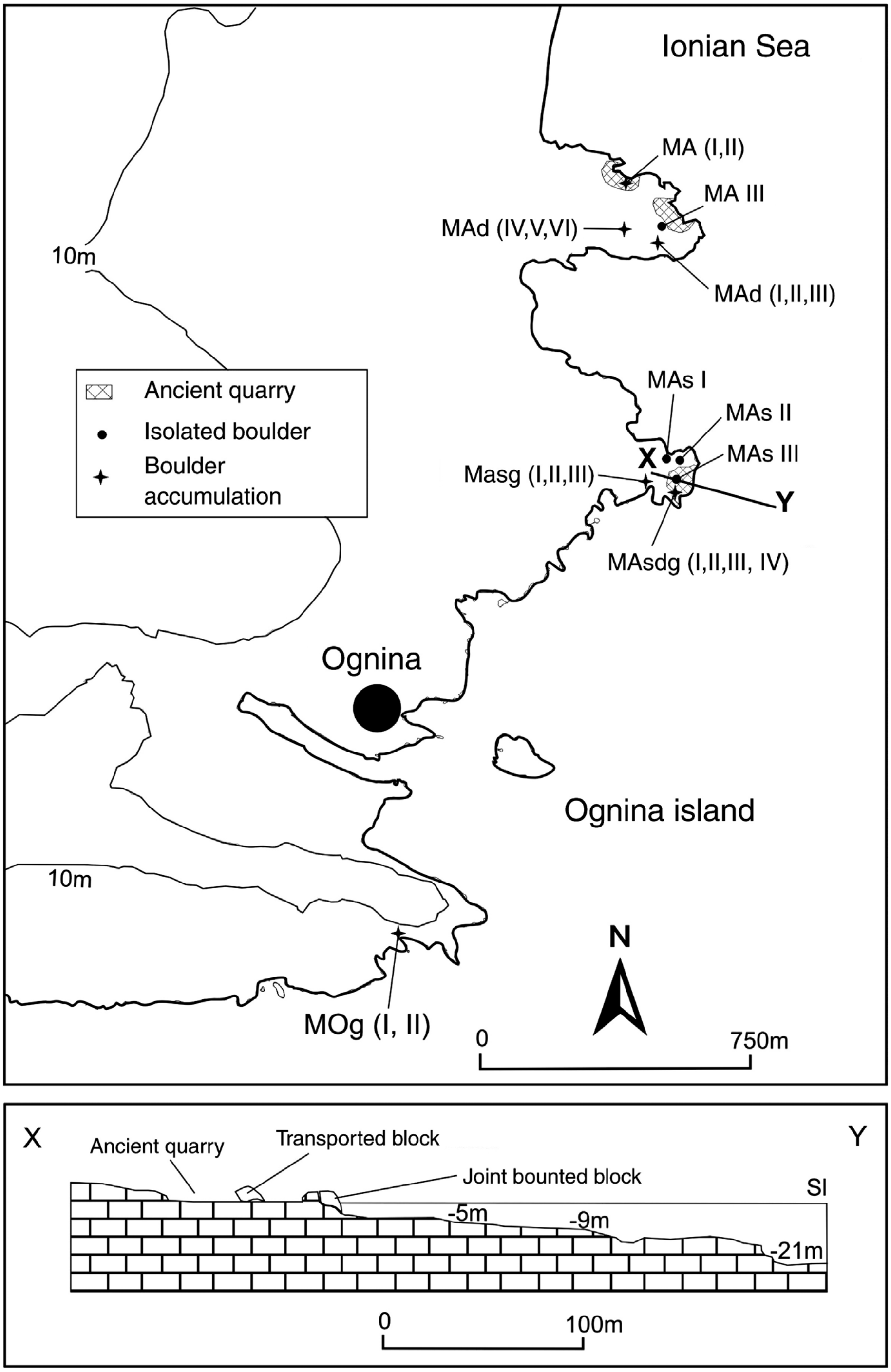

Fig. 8. Position of boulders surveyed at Ognina (see Fig. 2 for location) and submerged profile showing the near-shore sea bottom topography.

is evident that storm waves cannot be responsible for the deposition of many boulders surveyed in the Augusta–Siracusa area, being greater than 8.11–9.36 m the wave height necessary to detach and transport them (see Table 2). This suggests that the detachment and transport of the largest boulders could be the effect of the run-up of tsunami occurred in the past along the Augusta–Siracusa coastal area. In particular, tsunami waves would have been responsible for the detachment of the boulders MAg I in the Mt. Tauro Peninsula, MT I–VII, MT IX–X in the

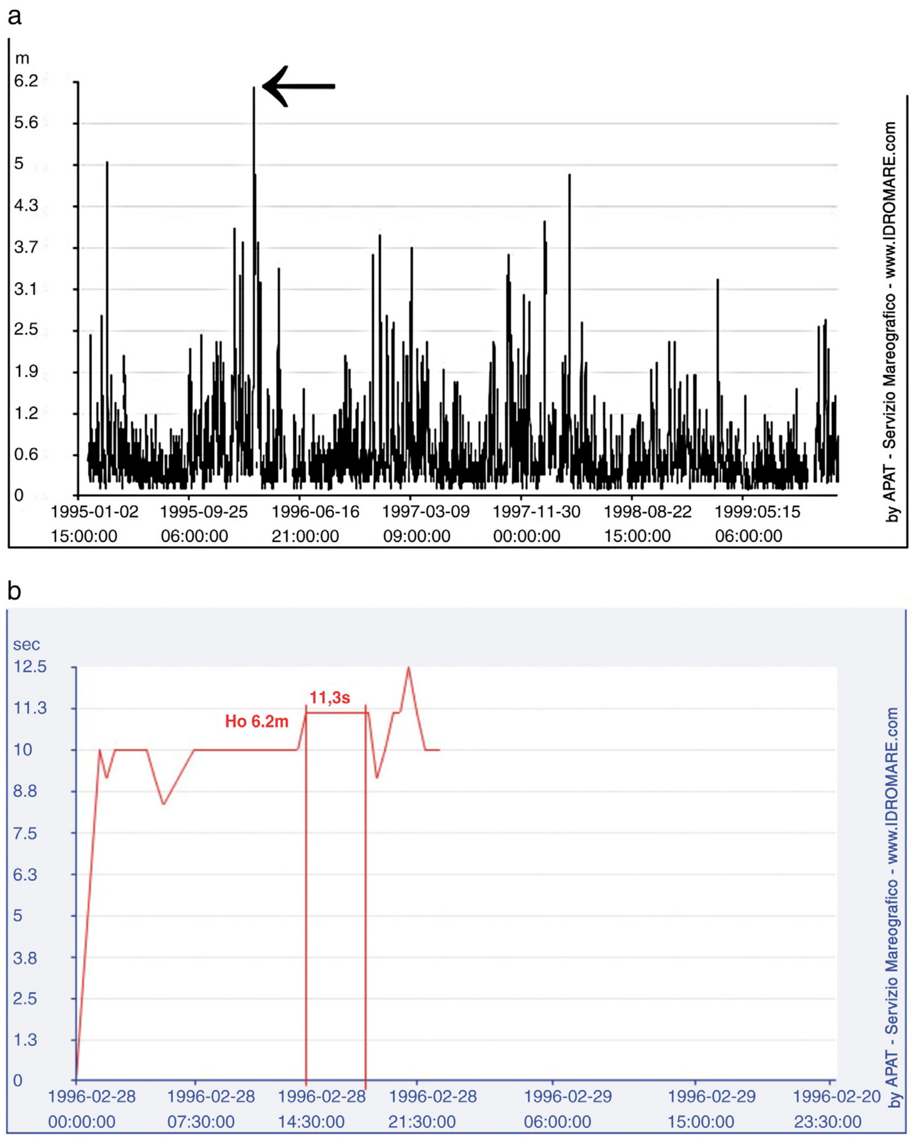

Fig. 9. Significant wave heights (H_o) recorded at Catania buoy (RON — Rete Ondametrica Nazionale; www.idromare.com) from 01/01/1995 to 31/12/2003 (a). The arrow indicates the maximum H_o (=6.2 m) occurred on February 2, 1996 which was characterized by a peak period T_p=11.3 s (b).

Magnisi Peninsula, B1–4, B8–9, B13, B17–19 in the Maddalena Peninsula and MA I–III, MAd I–VII, MAs II, MAsg II–III, MOg I–II in the Ognina site.

According to Noormets et al. (2002), boulders can be moved and re-oriented by other wave events post-deposition. As a matter of fact, many of the boulders detected in the Augusta–Siracusa coastal area (see for example B6 in the previous chapter) could have been transported to the shore platforms by tsunami waves and then moved again by extreme storm waves. A similar process has been described by Mastronuzzi and Sansò (2004) for boulders occurring along the Adriatic coast of southern Apulia. On the other hand, in many cases it would be compatible with the sub-aerial boulder scenario of Nott (2003a) according to which lower breaking waves are required to move sub-aerial blocks. To verify this possibility, the azimuthal angle of the *A*-axis (Table 2) has been compared to the azimuth distribution of the waves recorded by the Catania buoy of RON during the period 1989–2006 (Fig. 10). This diagram shows that the highest waves (H> 5 m) approached the studied coastal area from directions ranging between N70E and N110E with frequency peaks almost orthogonal to the *A*-axis orientation of most small-sized boulders (Table 2). This

Table 3
Different values of mean sea bottom slope (α) from −100 m depth to the shoreline, determined for the studied coastal sites along the mean direction of extreme waves (N100E)

Site	Sea bottom slope α (°)	$H_{o\ (RON)}$ (m)	T (s)	$L_{o\ (RON)}$ (m)	$H_{o\ (50)}$ (m)	$H_{b\ (RON)}$ (m)	$H_{b\ (50)}$ (m)
Mt. Tauro Peninsula	4.6	6.2	11.3	199.2	6.24	8.91	8.95
Magnisi Peninsula	2.6	6.2	11.3	199.2	6.24	8.11	8.15
Maddalena Peninsula	5.7	6.2	11.3	199.2	6.24	9.31	9.36
Ognina	2.6	6.2	11.3	199.2	6.24	8.11	8.15

In the table are also reported the wave height (H_o) and wave period (T) measured at deep water by the Catania buoy of the Rete Ondametrica Nazionale (RON; www.idromare.com), the estimated wave length ($L_o = gT^2/2\pi$; Sarpkaya and Isaacson, 1981), the wave height at deep water ($H_{o\ (50)}$) determined by statistical analysis (Inghilesi et al., 2000) for a return period of 50 years in the Catania sector, the different breaking wave heights at breaking points of the distinct sites ($H_{b\ (RON)}$ and $H_{b\ (50)}$). The latter were obtained processing respectively the RON data or the statistically determined values at deep water with the equation of Sunamura and Horikawa (1974).

suggests that storm waves could have been responsible for the movement and/or re-orientation of the small-sized blocks (characterized by $H_s < \sim 9$ m), possibly carved out and transported during previous tsunami waves. However, the largest boulders (characterized by $H_s > \sim 9$ m) should not have undergone remobilization as the required breaking waves exceed the storm regime of the analysed coastal area.

4.2. Comparison between dating results and tsunami catalogues

In order to relate the boulder accumulations to tsunami events occurred in the Augusta–Siracusa area, radiocarbon age determinations on marine biogenic encrustations collected from the largest boulders (Table 4) were compared to the most complete and updated tsunami catalogues for the Mediterranean area (e.g. Tinti et al., 2004). The calibration of radiocarbon determinations was carried out using the program Calib 5 (Stuiver and Reimer, 1993; Stuiver et al., 2005) for the marine environment with 402 years reservoir age.

As regards the Maddalena Peninsula, calendar ages of the boulders B2, B8 and B16 are 141–249 yr, 121–252 yr and 117–245 yr B.P., respectively (Table 4). The deposition of these boulders could be related to the "light" tsunami (Intensity = 2; Tinti et al., 2004; Table 1) generated by the February 20, 1818 earthquake ($M = 6$), whose source is located onshore in the eastern slope of Mt. Etna (Azzaro and Barbano, 2000), or to the "disastrous" tsunami of December 28, 1908 (Intensity = 6; Tinti et al., 2004; Table 1), generated by the $M_w = 7.1$ earthquake occurred offshore in the Messina Straits (Platania, 1909; Baratta, 1910; Tinti and Armigliato, 2003). It is worth to note that the H_t values estimated for these boulders (2.68 m, 2.86 m, 2.42 m, respectively, see Table 4) are well constrained by wave heights reported by Platania (1909) for the 1908 event, based on a field survey carried out in the weeks after the tsunami, and by Baratta (1910), who collected chronicles from several sources. According to Platania (1909) the wave reached a maximum height of 11 m in southern part of the Messina Straits, whereas to the south, in the Augusta area, waves were 1.75 m high. As regards the Siracusa area, Baratta (1910) quotes the reliable report of the Siracusa harbour office (*Regia Capitaneria di Porto*) that estimated a 2.0 m high wave, and other chronicles that reported values of 1.2–1.6 m. For this reason we prefer to relate deposition of these boulders to the 1908 tsunami. This event should be also responsible for deposition of the boulders B4 and B13 ($H_t = 3.04$ m and 2.63 m, respectively), whose calendar ages are younger than 95 years (Table 4).

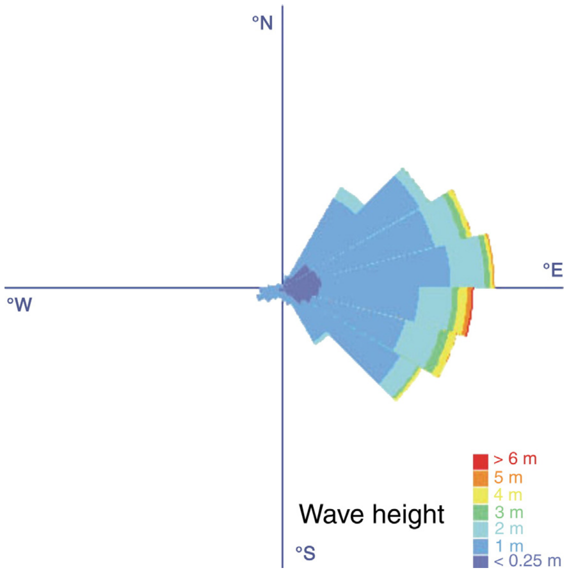

Fig. 10. Azimuth distribution and relative heights of waves recorded by the Catania buoy of Rete Ondametrica Nazionale (www.idromare.com) during the period 1989–2006.

Table 4
^{14}C AMS dating results of shell fragments collected from the boulders and analysed at the R.J. Van de Graaff laboratorium of the Utrecht University

Boulder	Site	Lab. number Utc	Analysed fraction	^{14}C age (BP)	Calendar age (yr cal BP)	H_t (m)	H_s (m)
MT IX	Magnisi Penins.	14086	*Serpulid*	1038±45	566–584	5.10	20.40
B2	Maddalena Penins.	14081	*Serpulid*	552±36	141–249	2.68	10.74
B4	Maddalena Penins.	12653	*Balanid*	465±37	0–95	3.04	12.16
B8	Maddalena Penins.	14082	*Serpulid*	539±44	121–252	2.86	11.45
B9	Maddalena Penins.	14083	*Serpulid*	960±41	517–570	9.37	37.50
B13	Maddalena Penins.	12655	*Balanid*	465±35	0–92	2.63	10.51
B16	Maddalena Penins.	14085	*Serpulid*	530±38	117–245	2.42	9.68
Mas II	Ognina	14087	*Serpulid*	1514±45	1003–1129	10.63	42.54

All samples were calibrated using the program Calib 5 (Stuiver and Reimer, 1993; Stuiver et al., 2005) for the marine environment with 402 years reservoir age. Tsunami and storm wave heights required for their transport according to the equations of Nott (2003a) are also reported.

Samples of *serpulids* collected on the boulder B9 (Maddalena Peninsula) and MT IX (Magnisi Peninsula) yielded calendar ages of 517–570 yr and 566–584 yr B.P., respectively (Table 4). Tentatively, we can attribute their deposition to the "very strong" tsunami occurred during the January 11, 1693 destructive earthquake (Intensity = 5; Tinti et al., 2004; Table 1), which was recorded all along the eastern coast of Sicily and in the island of Malta (Anonymous, 1693; Boccone, 1697; Bottone, 1718; Baratta, 1901; Piatanesi and Tinti, 1998; Tinti and Armigliato, 2003). For these blocks have been estimated values of H_t = 9.37 m and 5.10 m, which are compatible with the 12 m high tsunami wave reported by Boccone (1697) in the town of Augusta. Mesoseismic information and the characteristics of the tsunami suggest that the main shock may be related to rupture occurred along a normal fault located offshore (Barbano and Cosentino, 1981; Barbano, 1985; Bianca et al., 1999), which is consistent with the numerical modeling simulations performed by Tinti et al. (2001).

Finally, a calendar age of 1003–1129 yr B.P. has been determined for the boulder Mas II, found in the Ognina area (Table 4). Taking into account the Tsunami Catalogue of Tinti et al. (2004), its deposition could be related to the "strong" tsunami occurred during February 4, 1169 earthquake (Intensity = 4; Tinti et al., 2004; Table 1), whose intensity would be compatible with the H_t = 10.63 m estimated applying Nott's (2003a) equations. The analogies between the 1169 and the well-known 1693 event suggest a similar location and magnitude for both events (Lombardo, 1985; Azzaro and Barbano, 2000).

Location of offshore source areas of tsunamis along the active faults in the Messina Straits and at the foot of the Malta Escarpment (Fig. 1) is also suggested by preferential accumulation of boulders on sectors of promontories exposed towards the north-east (Fig. 2).

5. Conclusions

Ancient chronicles report that the Ionian coast of Sicily was struck by large tsunamis in historical times. Taking into account the high density of population living on the coastal plains, tsunamis represent one of the major factors of geological risk. In order to assess the effective hazard in terms of intensity and recurrence time, one approach is represented by identifying large boulders accumulated on shore platforms and determining wave heights and age of deposition. It was successfully applied in Australia (Nott, 1997, 2003a, b), Hawaii (Noormets et al., 2002, 2004), and Italy (Mastronuzzi and Sansò, 2000, 2004). In this study we carried out a detailed survey of large boulder accumulations along the Ionian coast of south-eastern Sicily which, combined with age determinations, allowed us to define the processes responsible for their formation and to underline their significance as indicators of catastrophic waves.

A hydrodynamic approach based on the equations proposed by Nott (2003a) has been used to determine whether tsunami- or storm-generated waves were responsible for coastal boulder deposition. Direct measurements of size and density of several boulders have been carried out to solve Nott's equations. The analysis suggests that tsunamis would be responsible for the detachment and transport of the largest blocks, which are incompatible with the storm wave regime of the studied area. It is not excluded that storm waves could have been responsible for the movement and/or re-orientation of small-sized blocks, possibly carved out and transported during previous tsunami waves. The analysis also confirms the importance of the pre-transport setting of boulders in determining the height of the wave required for it to be transported, as suggested by Nott (2003a), and that diffuse layering and fracturing of shore platform rocks favour the detachment of large blocks from the platform edge, as suggested by Noormets et al. (2004).

Radiocarbon age determinations on marine organisms encrusting the boulders, compared to historical catalogues, suggest that large tsunamis with local source have washed over the area at least three times in the last 1000 years. The first two tsunamis were probably triggered by the earthquakes of February 4, 1169 and January 11, 1693 which destroyed south-eastern Sicily. According to published geological data and numerical modelling, the seismogenic source could be located in the Ionian offshore between Catania and Siracusa along a large normal fault segment of the Siculo-Calabrian rift zone. The third tsunami was generated by the strong earthquake which took place in the Strait of Messina on December 28, 1908, where another normal fault segment was reactivated. For this event there is a good correspondence between measured wave heights and those estimated by Nott's equation.

Acknowledgements

This work was financed by the Project MIUR–PRIN "Analysis of the tsunami risk in Calabrian Arc and Adriatic Sea" (Resp. L. Tortorici). We thank the two anonymous reviewers and the Editors for their comments that helped to clarify some aspects of the work. We are grateful to A. Cannata for unit weight determination.

References

A.A.V.V., 1987. Carta Geologica della Sicilia sud-orientale. S.El.Ca., Firenze.

Adam, J., Reuther, C.D., Grasso, M., Torelli, L., 2000. Active fault kinematics and crustal stresses along the Ionian margin of southeastern Sicily. Tectonophysics 326, 217–239.

Anderson, H., Jackson, J., 1987. The deep seismicity of the Tyrrhenian Sea. Geophys. J. R. Astron. Soc. 91, 613–637.

Anonymous, 1693. Sincera ed esatta relazione dell'orribile terremoto seguito nell'Isola di Sicilia il di 11 di Gennaio 1693. Colla nota delle Città e Terre sprofondate, de' morti e luoghi che hanno patito, e con tutte le particolarità più degne da essere registrate. Roma.

Argnani, A., Bonazzi, C., 2005. Malta Escarpment fault zone offshore eastern Sicily: Pliocene–Quaternary tectonic evolution based on new multichannel seismic data. Tectonics 24, TC 4009. doi:10.1029/2004TC001656.

Azzaro, R., Barbano, S., 2000. Analysis of the seismicity of southeastern Sicily: a proposed tectonic interpretation. Ann. Geofis. 43, 171–188.

Baratta, M., 1901. I terremoti d'Italia. Arnaldo Forni, Bologna.

Baratta, M., 1910. La catastrofe sismica calabro-messinese (28 Dicembre 1908). Relaz. Soc. Geogr. Ital. Roma, 426 pp.

Barbano, S., 1985. The Val di Noto earthquake of January 11, 1693. In: Postpischl, D. (Ed.), Atlas of Isoseismal Maps of Italian Earthquake. PGF–CNR, Quaderno Ricerche Scientifiche, vol. 114 (2A), pp. 48–49.

Barbano, S., Cosentino, M., 1981. Il terremoto siciliano dell'11 Gennaio 1693. Rend. Soc. Geol. Ital. 4 (5), 517–522.

Bianca, M., Monaco, C., Tortorici, L., Cernobori, L., 1999. Quaternary normal faulting in southeastern Sicily (Italy): a seismic source for the 1693 large earthquake. Geophys. J. Int. 139, 370–394.

Boccone, P., 1697. Intorno al terremoto della Sicilia seguito l'anno 1693. Museo di Fisica, Venezia.

Boschi, E., Ferrari, G., Gasperini, P., Guidoboni, E., Smriglio, G., Valensise, G., 1995. Catalogo dei forti terremoti in Italia dal 461 a.c. al 1980. Istituto Nazionale di Geofisica, S.G.A., Roma.

Bottone, D., 1718. De immani Trinacriae terraemotu. Idea historico-physica, in qua non solum telluris concussiones transactae recensetur, sed novissimae anni 1717, Messina.

Bryant, E.A., 2001. Tsunami. The Underrated Hazard. Cambridge University Press, Cambridge. 320 pp.

Bryant, E.A., Nott, J.F., 2001. Geological indicators of large tsunami in Australia. Nat. Hazards 24, 231–249.

Carbone, S., Cosentino, M., Grasso, M., Lentini, F., Lombardo, G., Patanè, G., 1982. Elementi per una prima valutazione dei caratteri sismotettonici dell'Avampaese Ibleo (Sicilia sud-orientale). Mem. Soc. Geol. Ital. 24, 507–520.

Cello, G., Guerra, I., Tortorici, L., Turco, E., Scarpa, R., 1982. Geometry of the neotectonic stress field in southern Italy: geological and seismological evidence. J. Struct. Geol. 4, 385–393.

CMT Catalogne, 1976–2006. http://www.seismology.harvard.edu/CMTsearch.html.

D'Agostino, N., Selvaggi, G., 2004. Crustal motion along the Eurasia–Nubia plate boundary in the Calabrian Arc and Sicily and active extension in the Messina Straits from GPS measurements. J. Geophys. Res. 109, B11402.

Dawson, A.G., 1994. Geomorphological effects of tsunami run-up and backwash. Geomorphology 10, 83–94.

Dawson, A.G., Shi, S., 2000. Tsunami deposits. Pure Appl. Geophys. 157, 875–897.

Gasparini, C., Iannacone, G., Scandone, P., Scarpa, R., 1982. Seismotectonics of the Calabrian Arc. Tectonophysics 82, 267–286.

Ghisetti, F., 1992. Fault parameters in the Messina Strait (southern Italy) and relations with the seismogenic source. Tectonophysics 210, 117–133.

Grasso, M., Lentini, F., 1982. Sedimentary and tectonic evolution of the eastern Hyblean Plateau (southeast Sicily) during Late Cretaceous to Quaternary times. Palaeogeogr. Palaeoclimatol. Palaeoecol. 39, 261–280.

Heck, N.H., 1947. List of seismic sea waves. Bull. Seismol. Soc. Am. 37 (4), 269–286.

Inghilesi, R., Corsini, S., Guiducci, F., Arseni, A., 2000. Statistical analysis of extreme waves on the Italian coasts from 1989 to 1999. Boll. Geofis. Teor. Appl. 41 (3–4), 315–337.

Istituto Idrografico della Marina, 1998. Carta nautica del litorale di Augusta e Siracusa, F. 270. Marina Militare Italiana, Genova, Italy.

Jacques, E., Monaco, C., Tapponnier, P., Tortorici, L., Winter, T., 2001. Faulting and earthquake triggering during the 1783 Calabria seismic sequence. Geophys. J. Int. 147, 499–516.

Kelletat, D., Schellmann, G., 2002. Tsunami on Cyprus: field evidences and ^{14}C dating results. Z. Geomorphol., N.F. 46 (1), 19–34.

Lombardo, G., 1985. The Catania earthquake of February 4, 1169. In: Postpischl, D. (Ed.), Atlas of Isoseismal Maps of Italian Earthquake. PGF–CNR. Quaderno Ricerche Scientifiche, vol. 114 (2A), pp. 12–13.

Makris, J., Nicolich, R., Weigel, W., 1986. A seismic study in the western Ionian Sea. Ann. Geophys. 6, 665–678.

Mastronuzzi, G., Sansò, P., 2000. Boulders transport by catastrophic waves along the Ionian coast of Apulia (Southern Italy). Mar. Geol. 170, 93–103.

Mastronuzzi, G., Sansò, P., 2004. Large boulder accumulations by extreme waves along the Adriatic coast of southern Apulia (Italy). Quat. Int. 120, 173–184.

Monaco, C., Tapponier, P., Tortorici, L., Gillot, P.Y., 1997. Late Quaternary slip rates on the Acireale–Piedimonte normal faults and tectonic origin of Mt. Etna (Sicily). Earth Planet. Sci. Lett. 147, 125–139.

Monaco, C., Tortorici, L., 2000. Active faulting in the Calabrian arc and eastern Sicily. J. Geodyn. 29, 407–424.

Nakata, T., Kawana, T., 1993. Historical and prehistoric large tsunami in the southern Ryukyus, Japan. Tsunami, '93. Proceedings.

Noormets, R., Felton, E.A., Crook, K.A.W., 2002. Sedimentology of Rocky Shorelines: 2. Shoreline megaclasts on the north shore of Oahu, Hawaii: origins and history. Sediment. Geol. 150 (1–2), 31–45.

Noormets, R., Crook, K.A.W., Felton, E.A., 2004. Sedimentology of Rocky Shorelines: 3. Hydrodynamics of megaclast emplacement and transport on a shore platform, Oahu, Hawaii. Sediment. Geol. 172 (1–2), 41–65.

Nott, J., 1997. Extremely high-energy wave deposits inside the great barrier reef, Australia: determining the cause—tsunami or tropical cyclone. Mar. Geol. 141, 193–207.

Nott, J., 2003a. Waves, coastal boulder deposits and the importance of the pre-transport setting. Earth Planet. Sci. Lett. 210, 269–276.

Nott, J., 2003b. Tsunami or storm waves?—Determining the origin of a spectacular field of wave emplaced boulders using numerical storm surge and wave models and hydrodynamic transport equations. J. Coast. Res. 19, 348–356.

Nott, J., 2004. The tsunami hypothesis—comparison of the field evidence against the effects, on the Western Australian coast, of some of the most powerful storms on Earth. Mar. Geol. 208, 1–12.

Piatanesi, A., Tinti, S., 1998. A revision of the eastern Sicily earthquake and tsunami. J. Geophys. Res. 103, 2749–2758.

Platania, G., 1909. I fenomeni marittimi che accompagnarono il terremoto di Messina del 28 Dicembre 1908. Riv. Geogr. Ital. 3, 8 pp.

Postpischl, D., 1985. Catalogo dei terremoti italiani dall'anno 1000 al 1980, CNR, P.F. Geodinamica, Graficoop, Bologna. 239 pp.

RCMT Catalogue, 1997–2006. http://mednet.ingv.it/events/QRCMT/Welcome.html.

Sarpkaya, T., Isaacson, M., 1981. Mechanics of Wave Forces on Offshore Structures. Van Nostrand Reinhold Company Inc. 650 pp.

Sartori, R., Colalongo, M.L., Gabbianelli, G., Bonazzi, C., Carbone, S., Curzi, P.V., Evangelisti, D., Grasso, M., Lentini, F., Rossi, S., Selli, L., 1991. Note stratigrafiche e tettoniche sul rise di Messina (Ionio nord-occidentale). Giornale Geol. 53, 49–64.

Scandone, P., Patacca, E., Radoicic, R., Ryan, W.B.F., Cita, M.B., Rawson, M., Chezar, H., Miller, E., Mckenzie, J., Rossi, S., 1981. Mesozoic and Cenozoic rocks from Malta Escarpment (Central Mediterranean). A.A.P.G. Bull. 65, 1299–1319.

Scheffers, A., 2002. Paleotsunami in the Caribbean. Field evidences and datings from Aruba, Curacao and Bonaire. Essener Geographische Arbeiten, Band, vol. 33. Selbstverlag, Auflage-Essen. 186 pp.

Soloviev, S.V., 1990. Tsunamigenic zones in the Mediterranean Sea. Nat. Hazards 3, 183–202.

Soloviev, S.L., Solovieva, O.N., Go, C.N., Kim, K.S., Shchetnikov, N.A., 2000. Tsunamis in the Mediterranean Sea 2000 B.C.–2000 A.D. Kluwer Academic Publishers, Dordrecht. 237 pp.

Stuiver, M., Reimer, P.J., 1993. Extended ^{14}C data base and revised CALIB 3.0 ^{14}C age calibration program. In: Stuiver, M., Long, A., Kra, R.S. (Eds.), Calibration 1993. Radiocarbon, vol. 35 (1), pp. 215–230.

Stuiver, M., Reimer, P.J., Reimer, R., 2005. Calib radiocarbon calibration, execute version 5.0.2 html. http://calib.qub.ac.uk/calib2005.

Sunamura, T., Horikawa, K., 1974. Two dimensional beach transformation due to waves. Proceedings 14th Coastal Engineering Conference. American Society of Civilian Engineers, pp. 920–938.

Tinti, S., Armigliato, A., 2003. The use of scenarios to evaluate the tsunami impact in southern Italy. Mar. Geol. 199, 221–243.

Tinti, S., Armigliato, A., Bortolucci, E., 2001. Contribution of tsunami data analysis to constrain the seismic source: the case of the 1693 eastern Sicily earthquake. J. Seismol. 5, 41–61.

Tinti, S., Maramai, A., Graziani, L., 2004. The new catalogue of Italian tsunamis. Nat. Hazards 33, 439–465.

Tortorici, L., Monaco, C., Tansi, C., Cocina, O., 1995. Recent and active tectonics in the Calabrian arc (Southern Italy). Tectonophysics 243, 37–55.

Valensise, G., Pantosti, D., 1992. A 125 Kyr-long geological record of seismic source repeatability: the Messina Straits (southern Italy) and the 1908 earthquake (Ms 71/2). Terra Nova 4, 472–483.

Young, R.W., Bryant, E.A., Price, D.M., 1996. Catastrophic wave (tsunami?) transport of boulders in southern New South Wales, Australia. Z. Geomorphol., N.F. 40 (2), 191–207.

Ward, S.N., 1994. Constraints on the seismotectonics of the central Mediterranean from Very Long Baseline Interferometry. Geophys. J. Int. 117, 441–452.